

# Interactions of Macromolecules with Salt Ions: An Electrostatic Theory for the Hofmeister Effect

Huan-Xiang Zhou\*

Department of Physics and Institute of Molecular Biophysics and School of Computational Science, Florida State University, Tallahassee, Florida

**ABSTRACT** Salting-out of proteins was discovered in the nineteenth century and is widely used for protein separation and crystallization. It is generally believed that salting-out occurs because at high concentrations salts and the protein compete for solvation water. Debye and Kirkwood suggested ideas for explaining salting-out (Debye and MacAulay, *Physik Z*; 1925;131:22–29; Kirkwood, In: *Proteins, amino acids and peptides as ions and dipolar ions*. New York: Reinhold; 1943. p 586–622). However, a quantitative theory has not been developed, and such a theory is presented here. It is built on Kirkwood's idea that a salt ion has a repulsive interaction with an image charge inside a low dielectric cavity. Explicit treatment is given for the effect of other salt ions on the interaction between a salt ion and its image charge. When combined with the Debye-Hückel effect of salts on the solvation energy of protein charges (i.e., salting-in), the characteristic curve of protein solubility versus salt concentration is obtained. The theory yields a direct link between the salting-out effect and surface tension and is able to provide rationalizations for the effects of salt on the folding stability of several proteins. *Proteins* 2005;61:69–78. © 2005 Wiley-Liss, Inc.

**Key words:** Hofmeister effect; salting-out; protein solubility; protein stability; Debye-Hückel theory

## INTRODUCTION

In the nineteenth century it was discovered that various salts at high concentrations could precipitate proteins.<sup>1</sup> This salting-out effect has since been found to be a very general phenomenon, occurring not only on proteins but also on amino acids and even simple gas molecules.<sup>2,3</sup> A systematic study of salts on the solubility of hemoglobin was done by Green,<sup>4,5</sup> whose data are reproduced in Figure 1. These data show three characteristics: (1) an increase in solubility at low salt concentrations; (2) a decrease in solubility at high salt concentrations, with a linear slope; (3) the salting-out slope has a distinct order with respect to different types of salts, which is now known as the Hofmeister series. It is generally accepted that characteristic (1) arises from the Debye-Hückel effect on the solvation energy of the protein charges. However, the situations with characteristics (2) and (3) are much murkier.<sup>6</sup> Hofmeister<sup>1</sup> suggested that salting-out was due to dehydra-

tion of the protein by the added salt. This concept was reinforced by Debye and MacAulay<sup>7</sup> in arguing that the salt ions would attract the highly polar water molecules. Kirkwood<sup>8</sup> approached the salting-out problem on a sounder statistical mechanical basis. He too considered the interaction of a salt ion with the solvent and recognized that, when a salt ion is near a less polar protein molecule, an image charge is induced and a repulsive interaction between the salt ion and its image charge arises. Here we develop Kirkwood's idea further into a theory that qualitatively explains characteristics (1) and (2).

Kirkwood made calculations for the interaction of a salt ion with its image charge inside a low-dielectric spherical cavity. The model, shown in Figure 2(a), is closely related to one Kirkwood<sup>9</sup> and later Tanford and Kirkwood<sup>10</sup> used for calculating the solvation energy of protein charges. The major difference is that a protein charge is located inside the low-dielectric cavity, therefore interaction with its image charge in the solvent is attractive, whereas a salt ion is located in the high-dielectric solvent, thus interaction with its image charge in the cavity is repulsive. This unfavorable interaction energy is

$$u_{i0}(r_i) = \frac{e_i^2}{2r_i} \left( \frac{1}{\epsilon_p} - \frac{1}{\epsilon_s} \right) \sum_{l=1}^{\infty} \frac{l(R/r_i)^{2l+1}}{l + (l+1)\epsilon_s/\epsilon_p} \quad (1)$$

where  $R$  is the radius of the low-dielectric cavity,  $\epsilon_p$  and  $\epsilon_s$  are the low and high dielectric constants, and  $e_i$  and  $r_i$  are the charge and the radial distance of the salt ion. When other salt ions are present, the interaction energy will be strongly affected. An initial treatment of this effect, based on the linearized Poisson-Boltzmann (PB) equation and valid at low salt concentrations, has been presented previously.<sup>11</sup> Here extension to arbitrary salt concentrations is made through the use of the nonlinear PB equation. Such an extension is important because salting-out is mostly

The Supplementary Materials referred to in this article can be found at <http://www.interscience.wiley.com/jpages/0887-3585/suppmat/>

Grant sponsor: The National Institutes of Health; Grant number: GM58187.

\*Correspondence to: Huan-Xiang Zhou, Department of Physics and Institute of Molecular Biophysics and School of Computational Science, Florida State University, Tallahassee, FL 32306. E-mail: zhou@sb.fsu.edu

Received 6 January 2005; Revised 2 February 2005; Accepted 4 February 2005

Published online 25 July 2005 in Wiley InterScience ([www.interscience.wiley.com](http://www.interscience.wiley.com)). DOI: 10.1002/prot.20500

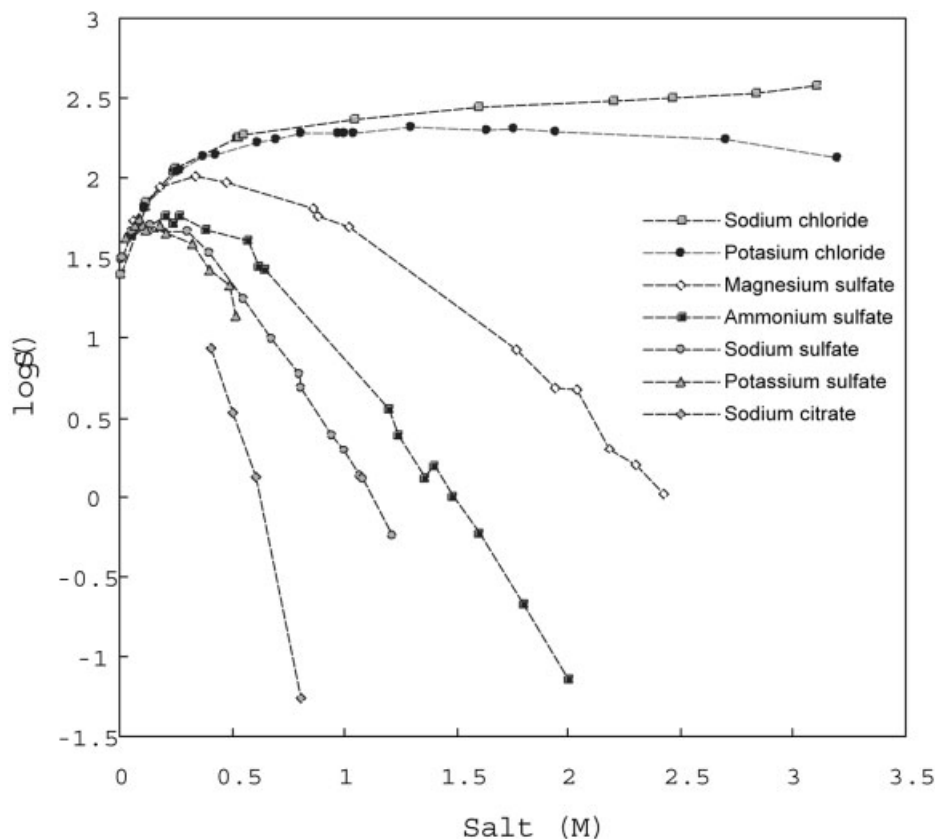


Fig. 1. Dependence of the solubility of horse carbonmonoxy hemoglobin on concentrations of seven salts. Lines are drawn to guide the eye through the data points, which are taken from Green.<sup>4,5</sup>

manifested at high salt concentrations. It should be noted that the PB equation is a mean field model with limitations such as the neglect of ion-ion correlations.

As is well known, the characteristics of salt effects on protein solubility are also seen on a wide range of other phenomena.<sup>12</sup> One such phenomenon is the increase in water-air surface tension by added salts. Onsager and Samaris,<sup>13</sup> following earlier work by Wagner,<sup>14</sup> explained the increase in surface tension,  $\Delta\gamma$ , as the result of depletion of salt ions near the water-air interface, due to the repulsion between the salt ions and their image charges.  $\Delta\gamma$  increases almost linearly with salt concentration. Here the use of the nonlinear PB equation is shown to improve predictions of surface-tension increase.

For a macromolecule with fixed charges embedded inside, the effects of mobile salt ions in the solvent can be formally divided into two contributions [Fig. 2(b)]. The first contribution is the work,  $w_{\text{out}}$  (for salting-out), to charge up the salt ions while the macromolecule is totally discharged. The second contribution is the work,  $\Delta w_{\text{in}}$  (for salting-in), to charge up the macromolecule in the presence of the fully charged salt ions. The salt ions change the chemical potential of the macromolecule, relative to the situation where no salt ions are present in the solvent, by

$$\Delta\mu = w_{\text{out}} + \Delta w_{\text{in}} \quad (2)$$

$\Delta w_{\text{in}}$  is negative because salt ions increase the magnitudes of the image charges of protein charges and thus strengthen their favorable interactions. This term accounts for the initial rise in protein solubility (i.e., salting-in).  $w_{\text{out}}$  is positive due to the repulsive interactions between salt ions and their image charges. The close connection between surface-tension increase and the “salting-out” work will be shown to be captured by an approximate relation,

$$w_{\text{out}} \approx (\Delta\gamma - k_{\text{B}}T\sigma\rho_0)A \quad (3)$$

where  $k_{\text{B}}T$  is the product of the Boltzmann constant and the absolute temperature,  $\sigma$  is the mean diameter of the salt ions,  $\rho_0$  is the salt concentration, and  $A$  is the surface area of the macromolecule. As the salt concentration increases, the magnitude of  $w_{\text{out}}$  increases more rapidly than that of  $\Delta w_{\text{in}}$ , leading to salting-out. It should be noted that there are also salts, notably those of iodide and thiocyanate ( $\text{SCN}^-$ ), that exhibit salting-in behavior at high concentrations.<sup>3,15</sup> The physical origin of this salting-in effect is distinct from that for  $\Delta w_{\text{in}}$  in Equation 2, and has been suggested to be some unknown “chaotropic” (i.e., water structure breaking) effect or favorable interactions with peptide groups. This second type of salting-in is outside the scope of the present theory.

At high concentrations, many salts are found to stabilize proteins, again with exceptions such as  $\text{SCN}^-$ .<sup>16–19</sup> The

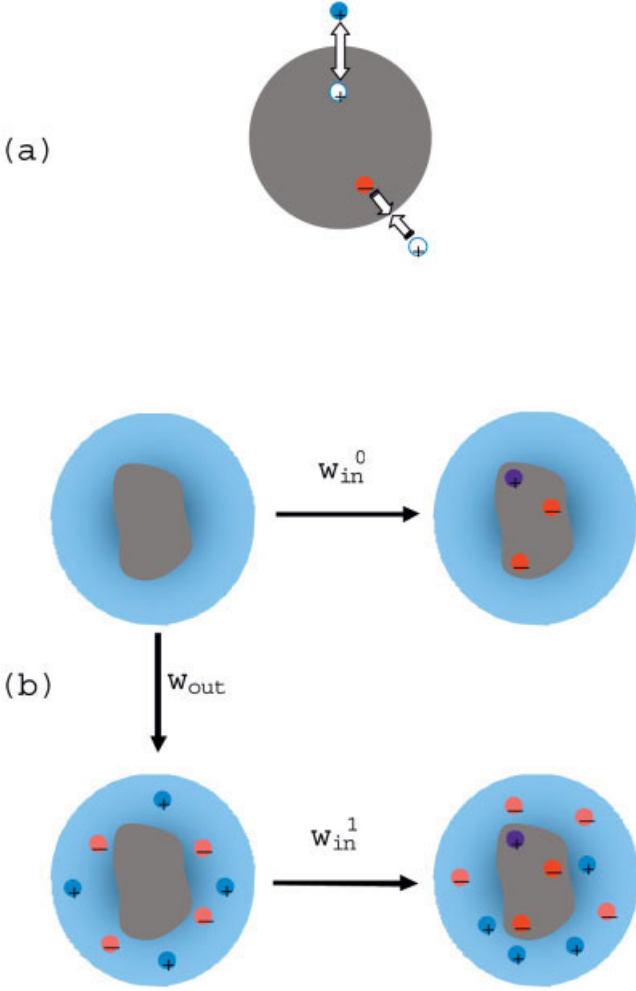


Fig. 2. Models for understanding the effects of protein charges and salt ions. **a:** A protein charge (shaded red), located in the low-dielectric cavity, induces an opposite image charge in the solvent and thus an attractive interaction (indicated by two approaching arrows). A salt ion (shaded blue), located in the high-dielectric solvent, induces a like image charge and thus a repulsive interaction (indicated by receding arrows). **b:** Electrostatic contributions to the chemical potential of a macromolecule (gray region at center) in the absence (upper horizontal arrow) and presence (vertical arrow followed by lower horizontal arrow) of salt ions. The vertical arrow gives  $w_{out}$ , while the difference between the two horizontal arrows gives  $\Delta w_{in}$  ( $= w_{in}^1 - w_{in}^0$ ). Note that salt ions in the solvent (shaded light blue) rearrange after the lower horizontal arrow.

stabilization is reminiscent of the salting-out effect. Indeed, as a protein molecule unfolds, the surface area and therefore the salting-out work increase, shifting the folding equilibrium toward the native state. Previously we compared the differential effects of salt on a mesophilic cold shock protein and its thermophilic counterpart.<sup>20</sup> As the salting-out work is expected to be nearly identical for the two homologous proteins, the differential effects of salt were explained by the salting-in work. When the salting-out work is now added to previously calculated results for salting-in, the sum is found to reproduce well experimental data<sup>17</sup> for the salt dependences of both cold shock proteins.

## THEORETICAL MODELS AND METHODS

### Electrostatic Potential of a Single Salt Ion

The electrostatic potential, at position  $\mathbf{r}$ , of a salt ion modeled as a point charge  $e_i$  located at  $\mathbf{r}_i$  satisfies the Poisson equation

$$\nabla \cdot \epsilon \nabla \phi_{i0}(\mathbf{r}|\mathbf{r}_i) = -4\pi e_i \delta(\mathbf{r} - \mathbf{r}_i) \quad (4)$$

where  $\epsilon = \epsilon_s$  in the solvent and  $\epsilon_p$  in the low-dielectric cavity. The boundary conditions are that  $\phi_{i0}(\mathbf{r}|\mathbf{r}_i)$  and the normal component of  $\epsilon \nabla \phi_{i0}(\mathbf{r}|\mathbf{r}_i)$  are continuous across the surface of the cavity. In the solvent one may write

$$\phi_{i0}(\mathbf{r}|\mathbf{r}_i) = \frac{e_s}{\epsilon_i |\mathbf{r} - \mathbf{r}_i|} + \varphi_{i0}(\mathbf{r}|\mathbf{r}_i) \quad (5a)$$

where the second term represents the potential due to the image charge inside the low-dielectric cavity. For a spherical cavity with radius  $R$ , it is simple to find that

$$\varphi_{i0}(\mathbf{r}|\mathbf{r}_i) = \frac{e_i}{R} \left( \frac{1}{\epsilon_p} - \frac{1}{\epsilon_s} \right) \sum_{l=1}^{\infty} \frac{l(R^2/r r_i)^{l+1} P_l(\cos \gamma)}{l + (l+1)\epsilon_s/\epsilon_p} \quad (5b)$$

where  $\gamma$  is the angle between  $\mathbf{r}$  and  $\mathbf{r}_i$  and  $P_l(x)$  are Legendre polynomials. The energy of interaction between the salt ion and its image charge is calculated as

$$u_{i0}(r_i) = e_i \varphi_{i0}(\mathbf{r}_i|\mathbf{r}_i)/2 \quad (6)$$

and the result is given in Equation 1. Note that  $\mathbf{r}_i$  is always located in the solvent. If on account of an ion exclusion radius the closest approach radius increases from  $R$  to  $R_i$ , then  $r_i > R_i$ .

### Effect of Other Salt Ions on the Electrostatic Potential

When other salt ions are present, each will contribute an analogous term  $\phi_{i'0}(\mathbf{r}|\mathbf{r}_{i'})$ . If the density of species  $i'$  salt ions around a *fixed* salt ion  $i$  is  $\rho_{i'}(\mathbf{r}|\mathbf{r}_i)$ , then the total electrostatic potential is

$$\phi_i(\mathbf{r}|\mathbf{r}_i) = \phi_{i0}(\mathbf{r}|\mathbf{r}_i) + \sum_{i'} \int d^3\mathbf{r}' \phi_{i'0}(\mathbf{r}|\mathbf{r}') \rho_{i'}(\mathbf{r}'|\mathbf{r}_i) \quad (7)$$

To make progress, one has to know the salt ion density  $\rho_{i'}(\mathbf{r}|\mathbf{r}_i)$ . Here we will make the Debye-Hückel approximation:

$$\rho_{i'}(\mathbf{r}|\mathbf{r}_i) = \rho_{i'0} \exp[-\beta e_{i'} \phi_i(\mathbf{r}|\mathbf{r}_i)] \quad \text{for } r > R_{i'} \text{ and } |\mathbf{r} - \mathbf{r}_i| > \sigma_{ii'} \quad (8a)$$

$$= 0 \quad \text{elsewhere} \quad (8b)$$

where  $\beta = (k_B T)^{-1}$  and  $\rho_{i'0}$  is the bulk concentration of species  $i'$ . Note that salt ions are not allowed to approach beyond  $\sigma_{ii'}$ , the distance of closest approach between salt ion  $i$  and species  $i'$ . For simplicity, all salt ions in the solvent will be assumed to have the same exclusion radius. The exclusion diameter will be simply denoted as  $\sigma$ , and the radius inside which salt ions are excluded will be denoted as  $R_i (= R + \sigma/2)$ . With Equation 4, it can be easily

shown that  $\phi_i(\mathbf{r}|\mathbf{r}_i)$  satisfies the nonlinear Poisson-Boltzmann equation

$$\nabla \cdot \varepsilon \nabla \phi_i(\mathbf{r}|\mathbf{r}_i) = -4\pi e_i \delta(\mathbf{r} - \mathbf{r}_i) - 4\pi \sum_{i'} e_{i'} \rho_{i'}(\mathbf{r}|\mathbf{r}_i) \quad (9)$$

Note that there are three distinct regions: in both  $r < R$  and  $R < r < R_i$  the source terms on the right-hand side are absent, but  $\varepsilon = \varepsilon_p$  in the former and  $\varepsilon_s$  in the latter; in  $r > R_i$  the source terms are present and  $\varepsilon = \varepsilon_s$ . At the boundaries  $r = R$  and  $r = R_i$ ,  $\phi_i(\mathbf{r}|\mathbf{r}_i)$  and the normal component of  $\varepsilon \nabla \phi_i(\mathbf{r}|\mathbf{r}_i)$  satisfy continuity conditions. We emphasize again that, for the present calculation, salt ion  $i$  is assumed to be fixed whereas all other salt ions are assumed to be mobile.

If the Boltzmann distribution in Equation 8(a) is expanded, and terms up to the first order are retained and assumed to be applicable even when  $|\mathbf{r} - \mathbf{r}_i| < \sigma$ , then one obtains the linearized PB equation:

$$\nabla \cdot \varepsilon \nabla \phi_{iL}(\mathbf{r}|\mathbf{r}_i) = -4\pi e_i \delta(\mathbf{r} - \mathbf{r}_i) + \varepsilon_s \kappa^2 M(\mathbf{r}) \phi_{iL}(\mathbf{r}|\mathbf{r}_i) \quad (10)$$

where the electrostatic potential is now denoted as  $\phi_{iL}(\mathbf{r}|\mathbf{r}_i)$ ,  $M(\mathbf{r})$  is a ‘‘masking’’ function that is 1 for  $r > R_i$  and 0 otherwise, and  $\kappa$  is the Debye-Hückel screening parameter given by

$$\kappa^2 = 4\pi\beta \sum_{i'} \rho_{i'} e_{i'}^2 / \varepsilon_s \quad (11)$$

The linearized PB equation can be solved analytically. The result can be expressed as

$$\phi_{iL}(\mathbf{r}|\mathbf{r}_i) = e_i g(\mathbf{r}|\mathbf{r}_i)$$

For  $r > R_i$  one has

$$g(\mathbf{r}|\mathbf{r}_i) = \frac{\exp(-\kappa|\mathbf{r} - \mathbf{r}_i|)}{\varepsilon_s |\mathbf{r} - \mathbf{r}_i|} + g_1(\mathbf{r}|\mathbf{r}_i) = \sum_{l=0}^{\infty} g_l(r; r_i) P_l(\cos \gamma) \quad (12a)$$

with

$$g_l(r_{<}; r_{>}) = \frac{2\kappa}{\pi \varepsilon_s} (2l + 1) [i_{l+1/2}(\kappa r_{<}) + A_l k_{l+1/2}(\kappa r_{<})] k_{l+1/2}(\kappa r_{>}) \quad (12b)$$

and

$$A_l = \frac{Y_l i_{l+1/2}(\kappa R_i) + (L_l + Y_l) \kappa R_i i_{l+3/2}(\kappa R_i) / (2l + 1)}{M_l k_{l+1/2}(\kappa R_i)} \quad (12c)$$

where

$$L_l = 1 + l + l \varepsilon_p / \varepsilon_s \quad (12d)$$

$$Y_l = (1 - \varepsilon_p / \varepsilon_s) l (R/R_i)^{2l+1} \quad (12e)$$

$$M_l = L_l + (L_l + Y_l) \kappa R_i k_{l-1/2}(\kappa R_i) / (2l + 1) k_{l+1/2}(\kappa R_i) \quad (12f)$$

and  $i_{l+1/2}(x)$  and  $k_{l+1/2}(x)$  are modified spherical Bessel functions.

The nonlinear PB equation has to be solved numerically. Here we chose to find  $\phi_i(\mathbf{r}|\mathbf{r}_i)$  by iterating an implicit equation starting from  $\phi_{iL}(\mathbf{r}|\mathbf{r}_i)$ . The desired implicit equation, for  $r > R_i$ , is

$$\begin{aligned} \phi_i(\mathbf{r}|\mathbf{r}_i) &= \phi_{iL}(\mathbf{r}|\mathbf{r}_i) - \int d^3 \mathbf{r}' g(\mathbf{r}|\mathbf{r}') \\ &\times \left[ - \sum_{i'} e_{i'} \rho_{i'}(\mathbf{r}'|\mathbf{r}_i) - (\varepsilon_s \kappa^2 / 4\pi) M(\mathbf{r}') \phi_i(\mathbf{r}'|\mathbf{r}_i) \right] \end{aligned} \quad (13)$$

Details of the solution are given in the Supplementary Online Material.

### Work of Charging up a Fixed Salt Ion

When the linearized PB equation is used, the work for charging up the fixed salt ion  $i$  at  $\mathbf{r}_i$  is

$$u_{iL}(r_i) = e_i^2 g_1(\mathbf{r}_i|\mathbf{r}_i) / 2 \quad (14)$$

When  $R_i \rightarrow R$ , Equation 14 reduces to a result derived previously.<sup>11</sup> With the nonlinear PB equation, one has to use a more general expression for the work, which can be derived through a charging process. It has been shown that three different processes lead to the same result for the work of charging up a fixed charge distribution.<sup>21</sup> The result for the fixed salt ion  $i$  is<sup>21,22</sup>

$$\begin{aligned} u_i(r_i) &= e_i \phi_i'(\mathbf{r}_i|\mathbf{r}_i) / 2 + \int_{|\mathbf{r}-\mathbf{r}_i|>\sigma} d^3 \mathbf{r} M(\mathbf{r}) \left\{ k_B T \sum_{i'} \rho_{i'} [1 \right. \\ &\left. - e^{-\beta e_i \phi_i(\mathbf{r}|\mathbf{r}_i)}] - \phi_i(\mathbf{r}|\mathbf{r}_i) \sum_{i'} e_{i'} \rho_{i'} e^{-\beta e_{i'} \phi_i(\mathbf{r}|\mathbf{r}_i)} / 2 \right\} \end{aligned} \quad (15)$$

where a prime indicates that an infinite term leading to the self-energy of the salt ion has been subtracted. The charging process of later interest is one in which the charges on both the fixed salt ion and all other salt ions are increased from zero to their respective full values. The other salt ions will redistribute in response to the charging process. The work expanded when all the charges are only a fraction  $\lambda$  of their full values will be denoted as  $u_i(r_i; \lambda)$ . The result in Equation 15 corresponds to  $\lambda = 1$ .

One may interpret  $u_i(r_i)$  as the potential of mean force of the fixed salt ion. The sign of  $u_i(r_i)$  will be positive because of the repulsive interaction with its image charge, while its magnitude will decrease with increasing  $r_i$ . One thus expects a depletion of salt ions near the surface of the low-dielectric cavity. The mean density of species  $i$  salt ions at  $r_i (> R_i)$  is given by

$$\Theta_i(r_i) = \rho_{i0} \exp[-\beta u_i(r_i)] \quad (16)$$

It is understood that any nonzero value of  $u_i(r_i)$  at infinite separation is to be subtracted from  $u_i(r_i)$ , so  $u_i(\infty) \rightarrow 0$ .

Throughout this work, unless otherwise indicated,  $\varepsilon_p$  was taken to be 4, and  $\varepsilon_s$  was assigned the value of the dielectric constant of water at the appropriate tempera-

ture (which is 78.5 at 25°C and 63.7 at 70°C). Though high salt concentrations are known to decrease the bulk dielectric constant of aqueous solutions,<sup>23</sup> given the depletion of salt ions near the macromolecular surface, the exact value of the dielectric constant there is uncertain. Such complications are avoided in this study.

### Work of Charging Up the Equilibrium Distribution of All Salt Ions

Consider again the process in which the charges on all salt ions are increased from zero to their respective full values. This time each salt ion is allowed to redistribute. Let us look at an intermediate step during this charging process, at which the charge of species  $i$  is  $\lambda e_i$ . When the charge is further increased by  $d\lambda e_i$  for each species, the additional work for charging up a salt ion that is of species  $i$  and located at  $\mathbf{r}$  is  $d\lambda \partial u_i(r; \lambda) / \partial \lambda$ .

Considering that the density of species  $i$  ions at  $\mathbf{r}$  is  $\Theta_i(r; \lambda)$ , the total work for charging up all salt ions in an equilibrium distribution is

$$\begin{aligned} w_{\text{out}} &= \int_0^1 d\lambda \sum_i \int d^3\mathbf{r} \Theta_i(r; \lambda) \frac{\partial u_i(r; \lambda)}{\partial \lambda} \\ &= \int_0^1 d\lambda \sum_i \int d^3\mathbf{r} \rho_{i0} M(\mathbf{r}) e^{-\beta u_i(r; \lambda)} \frac{\partial u_i(r; \lambda)}{\partial \lambda} \\ &= k_B T \sum_i \rho_{i0} \int d^3\mathbf{r} M(\mathbf{r}) [1 - e^{-\beta u_i(r)}] \quad (17) \end{aligned}$$

Note that the sum in Equation 17 is the total deficit of salt ions around the low-dielectric cavity.

### Work of Charging Up the Macromolecule: Spherical Boundary

The electrostatic potential  $\psi(\mathbf{r})$  originated from a fixed charge distribution inside the macromolecule,

$$\rho_p(\mathbf{r}) = \sum_j q_j \delta(\mathbf{r} - \mathbf{r}_j) \quad (18a)$$

satisfies the PB equation

$$\nabla \cdot \epsilon \nabla \psi(\mathbf{r}) = -4\pi \rho_p(\mathbf{r}) - 4\pi \sum_i e_i \rho_i(\mathbf{r}) \quad (18b)$$

where the density of the salt ions is

$$\rho_i(\mathbf{r}) = \rho_{i0} M(\mathbf{r}) \exp[-\beta e_i \psi(\mathbf{r})] \quad (18c)$$

The work for charging up the macromolecule is<sup>21,22</sup>

$$\begin{aligned} w_{\text{in}} &= \sum_j q_j \psi'(\mathbf{r}_j) / 2 + \int d^3\mathbf{r} M(\mathbf{r}) \left\{ k_B T \sum_i \rho_{i0} [1 - e^{-\beta e_i \psi(\mathbf{r})}] \right. \\ &\quad \left. - \psi(\mathbf{r}) \sum_i e_i \rho_{i0} e^{-\beta e_i \psi(\mathbf{r})} / 2 \right\} \quad (19) \end{aligned}$$

where a prime signifies elimination of the self-energy. The quantity  $\Delta w_{\text{in}}$  appearing in Equation 2 is the difference

between Equation 19 and its counterpart when salt ions are absent.

When the PB equation is linearized, the potential is given by<sup>9,10</sup>

$$\begin{aligned} \psi_L(\mathbf{r}) &= \sum_j \frac{q_j}{\epsilon_p |\mathbf{r} - \mathbf{r}_j|} - \left( \frac{1}{\epsilon_p} - \frac{1}{\epsilon_s} \right) \\ &\quad \sum_j \frac{q_j}{R} \sum_{l=0}^{\infty} \frac{(l+1)(r r_j / R^2)^l P_l(\cos \gamma_j)}{L_l} \\ &\quad - \sum_j \frac{q_j}{\epsilon_s R_i} \sum_{l=0}^{\infty} \frac{(2l+1) X_l(r r_j / R_i^2) P_l(\cos \gamma_j)}{L_l M_l} \quad (20) \end{aligned}$$

for  $r < R$ , where  $\gamma_j$  is the angle between  $\mathbf{r}$  and  $\mathbf{r}_j$  and  $X_l = \kappa R_i k_{l-1/2}(\kappa R_i) / k_{l+1/2}(\kappa R_i)$ . Note that the first two terms give the result in the absence of salt ions and the last term gives the contribution of the salt ions to  $\psi_L(\mathbf{r})$ . The work for charging up the macromolecule becomes

$$w_{\text{in;L}} = \sum_j q_j \psi'_L(\mathbf{r}_j) / 2 \quad (21)$$

The solution for  $r > R_i$  will become useful shortly, which can be written as

$$\psi_L(\mathbf{r}) = \sum_j q_j h(\mathbf{r} | \mathbf{r}_j) \quad (22a)$$

where

$$h(\mathbf{r} | \mathbf{r}_j) = \frac{1}{\epsilon_s R_i} \sum_{l=0}^{\infty} \frac{(2l+1)(r/R_i)^l k_{l+1/2}(\kappa r) P_l(\cos \gamma_j)}{M_l k_{l+1/2}(\kappa R_i)} \quad (22b)$$

Solution for  $\psi(\mathbf{r})$  was obtained by iteration starting from  $\psi_L(\mathbf{r})$ . The appropriate implicit equation is

$$\begin{aligned} \psi(\mathbf{r}) &= \psi_L(\mathbf{r}) - \int d^3\mathbf{r}' g(\mathbf{r} | \mathbf{r}') \\ &\quad \times \left[ - \sum_i e_i \rho_i(\mathbf{r}') - (\epsilon_s \kappa^2 / 4\pi) M(\mathbf{r}') \psi(\mathbf{r}') \right] \quad (23) \end{aligned}$$

For  $r > R_i$ ,  $\psi_L(\mathbf{r})$  is given by Equation 22(a) and  $g(\mathbf{r} | \mathbf{r}')$  is given by Equation 12(a). Once  $\psi(\mathbf{r})$  is obtained by iteration for  $r > R_i$ , it can be used in Equation 23 to calculate its values for  $r < R$ . In that region  $\psi_L(\mathbf{r})$  is given by Equation 20 and  $g(\mathbf{r} | \mathbf{r}')$  is the same as  $h(\mathbf{r}' | \mathbf{r})$ , which is given by Equation 22(b). Details of the solution are given in the Supplementary Online Material.

### Work of Charging Up the Macromolecule: Arbitrary Boundary

It was shown previously that the values of  $w_{\text{in}}$  calculated by the nonlinear and linearized PB equations were not significantly different.<sup>21</sup> The reason is that, given the large difference between  $\epsilon_s$  and  $\epsilon_p$ , the influences on the potential  $\psi(\mathbf{r})$  inside the macromolecule as modeled by the two versions of PB equation are comparable. The nonlinear

version slightly increases the magnitudes of the image charges of protein charges, making the first term in Equation 19 somewhat more negative. However, even this small change in the first term is partially offset by the addition of the second term in Equation 19, which is always positive. The solution of the nonlinear PB equation for a spherical macromolecule via Equation 23 allows for further comparison of the results for  $\Delta w_{in}$  calculated by the two versions of PB equation.

For realistic modeling of the salting-in work, the linearized PB equation with the actual shape and charge distribution of horse carbonmonoxy hemoglobin was solved numerically by the UHBD program.<sup>24</sup> The protocol follows our previous studies.<sup>20</sup> On the PDB entry 1g0b<sup>25</sup> hydrogen atoms were added and energy minimized by the CHARMM force field.<sup>26</sup> CHARMM charges were assigned to protein atoms. Around the pH ( $\sim 6.6$ ) where the solubility was found to be minimal and its salt dependences were measured,<sup>4,5</sup> hemoglobin has a net charge close to zero (with 58 Asp and Glu residues balanced by 58 Lys and Arg residues, but with some of the 28 His residues at least partially charged). The boundary of the low dielectric cavity was taken as the outer van der Waals surface of the protein molecule. Any voids inside the outer van der Waals surface were assigned the low dielectric constant. The electrostatic potential  $\psi_L(\mathbf{r})$  was calculated first on a  $100 \times 100 \times 100$  grid with a 1.5-Å spacing and then on a  $140 \times 140 \times 140$  grid with a 0.5-Å spacing.

In our previous work,<sup>20</sup> results of  $w_{in;L}$  for two cold shock proteins using their actual shapes and charge distributions were calculated. These are used here to predict the total effect of salts on the folding stability.

## RESULTS AND DISCUSSION

### Potential of Mean Force of a Salt Ion Around a Low-Dielectric Cavity

Figure 3(a) shows the potential of mean force,  $u_i(r_i)$ , of a salt ion in a 1 M 1:1 salt with an exclusion diameter of 4 Å outside a 16-Å spherical cavity at 25°C. The value of  $u_i(r_i)$  is  $\sim 0.4 k_B T$  at contact and extends about 6 Å. In comparison, the potential of mean force,  $u_{iL}(r_i)$ , calculated by the linearized PB equation has a slightly higher contact value ( $\sim 0.5 k_B T$ ) but decays more rapidly.

### Determinants of $w_{out}$

The integration of  $1 - \exp[-\beta u_i(r_i)]$  gives the salting-out work  $w_{out}$  (Equation 17). For the case shown in Figure 3(a),  $w_{out}$  is  $3.06 k_B T$ . If the linearized PB were used,  $w_{out}$  would be underestimated by  $\sim 21\%$ . The underestimate grows with salt concentration.

The value of  $w_{out}$  shows a nearly linear increase with salt concentration  $\rho_0$ , except at low  $\rho_0$ . Overall, the salt dependence can be fitted to [Fig. 3(b)]

$$\beta w_{out} = a \rho_0^{1/2} + b \rho_0 \quad (24)$$

For the 1:1 salt with  $\sigma = 4$ -Å outside a 16-Å spherical cavity, the fitting parameters are  $a = 1.04$  and  $b = 2.00$  when the salt concentration is in moles ( $\beta w_{out}$  is dimensionless). Reducing the exclusion diameter of the 1:1 salt

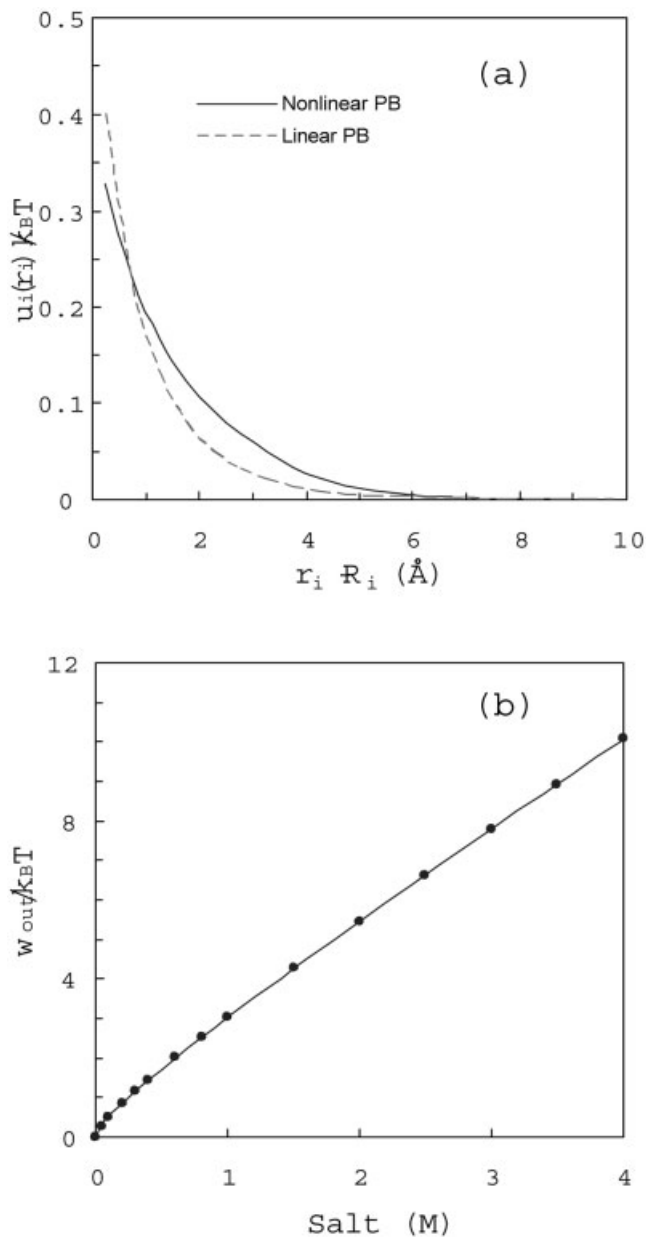


Fig. 3. **a**: The potential of mean force of an ion in a 1:1 salt with  $\sigma = 4$  Å at 1 M. The cavity radius is 16 Å. **b**: The dependence of the salting-out work on salt concentration for the 1:1 salt with  $\sigma = 4$  Å. The curve is a fit according to Equation 24.

results in an increase in  $w_{out}$ . At  $\sigma = 3$  Å, the fitting parameters become  $a = 1.28$  and  $b = 1.94$ . From the results at  $\sigma = 3$  and 4 Å, one may obtain values of  $w_{out}$  at other exclusion diameters by interpolation or extrapolation. In particular, the interpolated fitting parameters for  $\sigma = 3.5$  Å are  $a = 1.16$  and  $b = 1.97$ . At a higher temperature, the dielectric constant of water decreases, leading to an increase in  $w_{out}$ . At 70°C, the interpolated fitting parameters for  $\sigma = 3.5$  Å rise to  $a = 1.22$  and  $b = 2.01$ . Later, KCl and NaCl will be modeled as 1:1 salts with exclusion diameters of 4 and 3.5 Å, respectively.

As may be expected,  $w_{\text{out}}$  increases with the charge  $e_i$  on the salt ions. For a hypothetical  $3^{1/2}:3^{1/2}$  salt with  $\sigma = 4 \text{ \AA}$ , which mimics a 1:2 salt such as  $\text{Na}_2\text{SO}_4$ , the fitting parameters become  $a = 1.33$  and  $b = 5.12$  at  $25^\circ\text{C}$ . The value of  $w_{\text{out}}$  increases linearly with the surface area of the low-dielectric cavity.

### Magnitude of $\Delta w_{\text{in}}$ : Modest Difference Between Nonlinear and Linearized PB

In a previous study, it was found that the nonlinear and linearized PB equations do not predict significantly different results in  $\Delta w_{\text{in}}$  for typical proteins.<sup>21</sup> This finding is confirmed in the present work for spherical macromolecules. For example, for a macromolecule with a  $16\text{-\AA}$  radius in a  $0.1 \text{ M}$  1:1 salt at  $25^\circ\text{C}$ , when 25 positive unit charges and 24 negative unit charges are randomly distributed on a interior shell  $2 \text{ \AA}$  from the surface,  $\Delta w_{\text{in}}$  is  $-2.32 k_{\text{B}}T$  according to the nonlinear PB equation and  $-2.17 k_{\text{B}}T$  according to the linearized equation. When there are 40 unit positive charges and 30 unit negative charges,  $\Delta w_{\text{in}}$  becomes  $-16.9 k_{\text{B}}T$  and  $-15.6 k_{\text{B}}T$ , respectively, according to the two versions of PB equation. Increasing the ionic strength further reduces the relative difference between the two calculations of  $\Delta w_{\text{in}}$ .

The modest difference between the nonlinear and linearized PB estimates of  $\Delta w_{\text{in}}$  is in contrast to what is found for  $w_{\text{out}}$ . The disparity can be attributed to the fact that the source for  $\Delta w_{\text{in}}$ , i.e., the protein charges, resides in the low-dielectric cavity, whereas the source for  $w_{\text{out}}$ , i.e., the salt ions, resides in the high-dielectric solvent. For the results presented below,  $\Delta w_{\text{in}}$  was obtained by solving the linearized PB equation with the actual shapes and charge distributions of particular proteins.

### Effects of Different Salts on the Solubility of Hemoglobin

When the solution phase and crystalline phase of a protein come to equilibrium, the protein concentration in the solution is the solubility. The solubilities in the presence and absence of salt ions,  $S$  and  $S_0$ , respectively, are related to the change in chemical potential of the protein,  $\Delta\mu$  of Equation 2, via

$$-k_{\text{B}}T \ln(S/S_0) = \Delta\mu = w_{\text{out}} + \Delta w_{\text{in}} \quad (25)$$

which assumes that the chemical potential in the crystalline phase is not affected by salts.<sup>27</sup> In applying Equation 25,  $w_{\text{out}}$  for a particular protein was obtained by scaling the result for a  $16\text{-\AA}$  cavity with an adjustable effective radius  $R_{\text{eff}}$ :

$$w_{\text{out}} = w_{\text{out}}(16 \text{ \AA})(R_{\text{eff}}/16)^2 \quad (26)$$

but  $\Delta w_{\text{in}}$  was calculated through the linearized PB equation using the actual protein shape and charge distribution.

Figure 4 shows the calculated changes in hemoglobin solubility by three salts: NaCl, KCl, and  $\text{Na}_2\text{SO}_4$ . To avoid complications due to small errors caused by using the linearized PB equation for calculating  $\Delta w_{\text{in}}$  (see above) and possible salt ion binding to the protein,<sup>18</sup> only results

at salt concentrations higher than  $0.1 \text{ M}$  are presented. Qualitative agreement with the experimental data of Green<sup>4,5</sup> is obtained for all the three salts when the effective radius  $R_{\text{eff}}$  is taken as  $23.2 \text{ \AA}$ .

### Surface-Tension Increases by Different Salts

The low-dielectric cavity is equivalent to an air bubble. When the radius  $R \rightarrow \infty$ , the surface of the cavity become an infinite flat air-water interface. Technically it is more appropriate to assign a dielectric constant of 1 to air. However, as Onsager and Samaris<sup>13</sup> noted, the dependence of the salting-out work has only a weak dependence on  $\epsilon_{\text{p}}$  (due to the large  $\epsilon_{\text{s}}/\epsilon_{\text{p}}$  ratio). Indeed Onsager and Samaris carried out their calculations specifically for  $\epsilon_{\text{p}} = 0$ , for which the mathematics is significantly simplified. Calculations here with the spherical cavity also confirmed the very weak dependence of  $w_{\text{out}}$  on  $\epsilon_{\text{p}}$ .

Qualitatively, the positive potentials of mean force of salt ions around the low-dielectric cavity lead to a deficit around the cavity (Equation 17). This deficit in turn results in an increase in surface tension. If the total deficit of salt ions per unit surface area is  $\Gamma$ , then the surface tension  $\gamma$  can be determined from<sup>28</sup>

$$d\gamma = \Gamma d\mu_i \quad (27)$$

where  $\mu_i$  is the mean chemical potential of the salt ions. Neglecting the contribution of the activity coefficient of salt ions, one has

$$\mu_i \approx k_{\text{B}}T \ln \rho_0 \quad (28)$$

Integrating Equation 27, one obtains for the surface-tension increase

$$\Delta\gamma = k_{\text{B}}T \int_0^{\rho_0} (\Gamma/\rho_0) d\rho_0 \quad (29)$$

Equation 17 gives the deficit of salt ions for  $r > R_i = R + \sigma/2$ . It should be noted that salt ions are completely excluded between  $R$  and  $R_i$ . This salt-free layer also contributes to the deficit of salt ions. The contribution of the salt-free layer has been widely invoked.<sup>29–32</sup> The deficit of salt ions per unit area due to the salt-free layer amounts to  $\sigma\rho_0$ . Together with Equation 17, one has

$$\Gamma = \sigma\rho_0 + \beta w_{\text{out}}/A \quad (30)$$

where  $A = 4\pi R^2$  is the surface area of the spherical cavity. Note that since  $\beta w_{\text{out}}$  increases linearly with  $A$ , the ratio  $\beta w_{\text{out}}/A$  is independent of the size of the cavity. For concreteness, calculations of  $\delta\gamma$  were made using the results for the  $16\text{-\AA}$  cavity. With the salt dependence of  $\beta w_{\text{out}}$  given in Equation 24, one obtains

$$\Delta\gamma = k_{\text{B}}T[\sigma\rho_0 + (2a\rho_0^{1/2} + b\rho_0)/A] \quad (31a)$$

$$\approx k_{\text{B}}T[\sigma\rho_0 + \beta w_{\text{out}}/A] \quad (31b)$$

Rearrangement of Equation 31(b) leads to the result given in Equation 3.

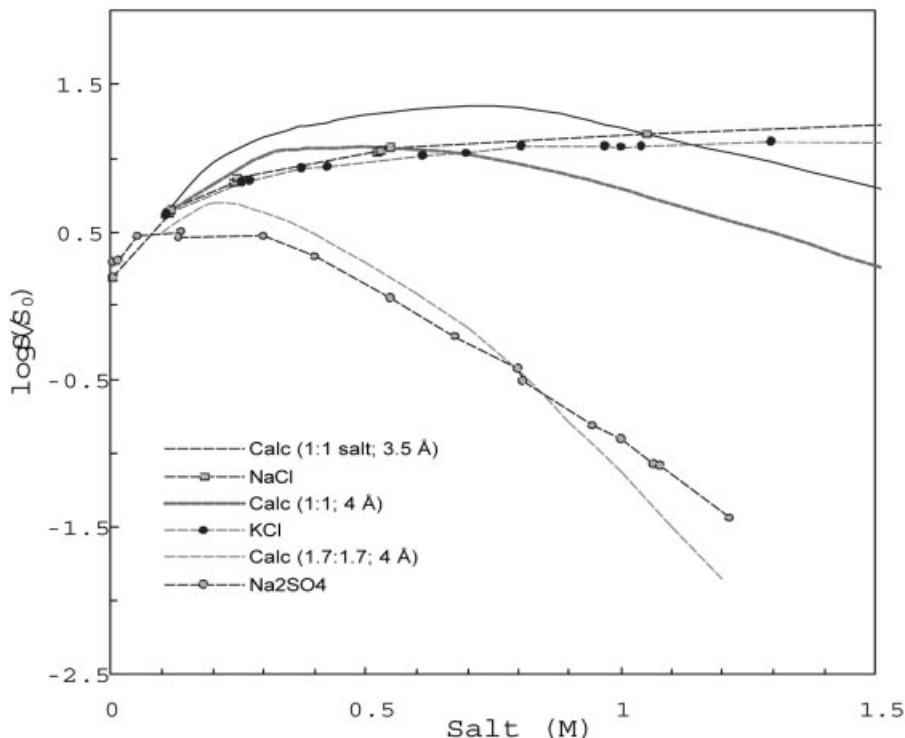


Fig. 4. Solubility of hemoglobin calculated according to Equation 25.  $\Delta w_{in}$  was calculated by numerically solving the linearized PB equation with the actual shape and charge distribution of hemoglobin.  $w_{out}$  was obtained from the result for a 16-Å cavity by scaling according to Equation 26, with  $R_{eff} = 23.2$  Å. NaCl and KCl were modeled as 1:1 salts with exclusion diameters of 3.5 and 4 Å, respectively;  $Na_2SO_4$  was modeled as a symmetric salt with charges  $\pm 3^{1/2}e$  and an exclusion diameter of 4 Å. The results at 0.1 M salts were used as reference. Experimental data are as shown in Figure 1.

Using the values of the fitting parameters  $a$  and  $b$  listed earlier, the surface-tension increases are found to be 1.42, 1.51, and 1.99 dynes/cm, respectively, at 1 M solutions of NaCl, KCl, and  $Na_2SO_4$ . The corresponding experimental data are 1.6–2.1, 1.6–1.9, and 2.9–3.0 dynes/cm.<sup>33,34</sup> The present study improves the work of Onsager and Samaris<sup>13</sup> in two respects: (1) the salt-free layer is explicitly taken into consideration; (2) the nonlinear PB equation instead of the linearized version is used. The first improvement was also made in the recent work of Ohshima and Matsubara.<sup>32</sup> The use of the nonlinear PB equation here moves electrostatic theories of surface tension one step further. The remaining discrepancy with experimental data perhaps can be attributed to lost dispersion interactions suffered by salt ions when they are near the air-water interface (in bulk solution each salt ion is surrounded by the solvent in all directions; not so when it is near the interface).<sup>35</sup>

### Effects of NaCl on the Stabilities of Cold Shock Proteins

When a protein is unfolded by denaturation, salt ions will affect the native and denatured states differently, resulting in a shift in the folding equilibrium. The change in free energy in one mole of protein molecules by salt ions in either the native or denatured state is

$$\Delta G^\alpha = \Delta \mu^\alpha = w_{out}^\alpha + \Delta w_{in}^\alpha \quad (32)$$

where the superscript  $\alpha = N$  for the native and D for the denatured states. The second term,  $\Delta w_{in}^\alpha$ , has been specifically studied in previous work.<sup>20</sup> In the native state,  $A_{in}^N$  is the difference in the work of charging up a folded protein molecule in the presence and absence of salt ions. The denatured state has been modeled as individually solvated residues plus residual electrostatic interactions between charged residues.<sup>20,36</sup>

$$\Delta w_{in}^D = \sum \Delta w_{in}(\text{residue}) + \sum \Delta w_{in}(\text{interaction}) \quad (33)$$

Only charged residues are included in the calculation of  $\Delta w_{in}^D$ . For calculating  $w_{in}(\text{residue})$ , a charged residue is carved from the folded molecule and solvated. The residual interaction energy,  $w_{in}(\text{interaction})$ , between two charged residues in the denatured state, is calculated as the average of the Debye-Hückel interaction potential between two point charges,

$$\Delta w_{in}(\text{interaction}) = \frac{q_i q_{j'}}{\epsilon_s r_{ij'}} e^{-\kappa r_{ij'}} \quad (34)$$

over a Gaussian distribution for the residue-residue distance  $r_{ij'}$ .

Results of  $\Delta w_{in}^N$  and  $\Delta w_{in}^D$  for a pair of cold shock proteins, Bc-Csp and Bs-CspB, have been presented in our previous study.<sup>20</sup> These two proteins differ in only 11 of 66 positions, with Bc-CspB also having an extra residue at the C terminal. The net charges at pH 7 are very different,  $-2e$

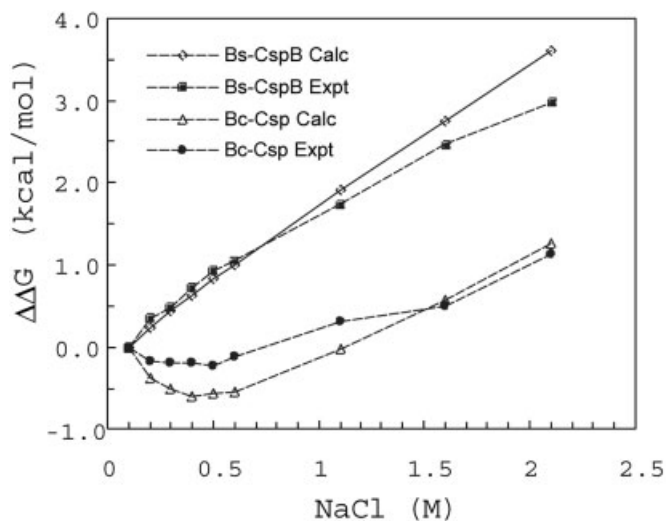


Fig. 5. Effects of NaCl on the unfolding free energies of two cold shock proteins (Bc-Csp and Bs-CspB) at 70°C. Experimental data are taken from Perl and Schmid.<sup>17</sup>

for Bc-Csp and  $-6e$  for Bs-CspB. It was assumed that the salting-out contribution

$$\Delta G_{\text{out}} = w_{\text{out}}^{\text{D}} - w_{\text{out}}^{\text{N}}$$

to the unfolding free energy is identical for the two homologous proteins. The differential effects of NaCl on the unfolding free energies of the two proteins, measured by Perl and Schmid,<sup>17</sup> were rationalized by the salting-in contribution

$$\Delta \Delta G_{\text{in}} = \Delta w_{\text{in}}^{\text{D}} - \Delta w_{\text{in}}^{\text{N}}$$

A main cause for the differential effects of NaCl on the folding stabilities was attributed to the difference in net charges.<sup>20,37</sup>

The  $\Delta G_{\text{out}}$  term can now be calculated. For this purpose, the folded molecule is modeled as a cavity with an effective radius  $R_{\text{eff}}$  and  $w_{\text{out}}^{\text{N}}$  is evaluated according to Equation 26. For the denatured state, each residue (charged or neutral) is modeled as a small cavity, with an effective radius  $r_{\text{eff}}$ . The total salting-out work in the denatured state is

$$w_{\text{out}}^{\text{D}} = n_{\text{res}} w_{\text{out}} (16 \text{ \AA}) (r_{\text{eff}}/16)^2 \quad (35)$$

where  $n_{\text{res}}$  is the number of residues in the protein. With  $R_{\text{eff}} = 11.5 \text{ \AA}$  and  $r_{\text{eff}} = 2.4 \text{ \AA}$ , it is possible to reproduce well the experimental salt dependences of the unfolding free energies of both cold shock proteins (Fig. 5). Since the denatured state has a larger surface area ( $n_{\text{res}} r_{\text{eff}}^2 > R_{\text{eff}}^2$ ), the salting-out work favors the native state and ultimately leads to its stabilization. A similar calculation with  $R_{\text{eff}} = 16 \text{ \AA}$  and  $r_{\text{eff}} = 2.4 \text{ \AA}$  has been found to reproduce experimental data for the effect of KCl on the stability of the 107-residue FK506 binding protein.<sup>38</sup>

## CONCLUSIONS

We have developed an electrostatic theory for the interactions of macromolecules with salt ions. Salt ions are

found to have two opposing effects on the chemical potential of the macromolecule. A salting-in effect arises because salt ions strengthen the favorable interactions between macromolecular charges with the solvent. A salting-out effect arises because salt ions induce repulsive interactions with image charges inside the low-dielectric macromolecular cavity. Two kinds of experimental data are analyzed: protein solubility and stability. Rationalizations are provided in both cases. A direct link between salting-out and surface-tension increase is also obtained.

Do interactions other than the electrostatic type considered here also play important roles? In considering surface-tension increase by salt ions, lost dispersion interactions near air-water interface have been implicated. However, around a macromolecular surface, lost dispersion interactions with solvent are replaced by gained dispersion interactions with the macromolecule. Thus to a crude approximation the loss and gain cancel each other and there is no net effect from dispersion interactions. However, the cancellation may not be complete and there could be subtle effects from dispersion interactions. These subtle effects may well be specific to each ion species and therefore contribute to the ordering of the Hofmeister series [characteristic (3) listed in Introduction]. In particular, anions such as  $\text{I}^-$  and  $\text{SCN}^-$  appear to have excessive “salting-in” effects.<sup>3,15</sup> These have been attributed to a chaotrope mechanism or to favorable interactions with peptide groups.

The electrostatic theory for salt ions developed here is based on a continuum solvent model. Molecular dynamics simulations with explicit water are providing insights on the details of the interactions of salt ions with water and macromolecules.<sup>39–44</sup> These insights may spur further theoretical developments for the effects of salt ions.

In conclusion, the electrostatic theory presented here may find applications in understanding the effects of salt ions on a wide range of properties of proteins, including aggregation, crystallization, and halophilicity.

## ACKNOWLEDGMENTS

I thank Robert L. Baldwin for discussion. This work was supported in part by NIH grant GM58187.

## REFERENCES

- Hofmeister F. Zur Lehre von der Wirkung der Salze. *Zweite Mittheilung. Arch Exp Pathol Pharmacol* 1888;24:247–260.
- Cohn EJ, Ferry JD. Interactions of proteins with ions and dipolar ions. In: Cohn EJ and Edsall JT, editors. *Proteins, amino acids and peptides as ions and dipolar ions*. New York: Reinhold Publishing Corporation; 1943. p 586–622.
- Nandi PK, Robinson DR. Effects of salts on the free energy of the peptide group. *J Am Chem Soc* 1972;94:1299–1308.
- Green AA. Studies in the physical chemistry of the proteins. VIII. The solubility of hemoglobin in concentrated salt solutions. A study of the salting-out of proteins. *J Biol Chem* 1931;93:495–516.
- Green AA. Studies in the physical chemistry of the proteins. X. The solubility of hemoglobin in chlorides and sulphates of varying concentration. *J Biol Chem* 1932;95:47–66.
- Baldwin RL. How Hofmeister ion interactions affect protein stability. *Biophys J* 1996;71:2056–2063.
- Debye P, MacAulay IJ. Das Elektrische Feld Der Ionen Und Die Neutralsalzwirkung. *Physik Z* 1925;131:22–29.
- Kirkwood JG. The theoretical interpretation of the properties of

- solutions of dipolar ions. In: Cohn EJ, Edsall JT, editors. *Proteins, amino acids and peptides as ions and dipolar ions*. New York: Reinhold Publishing Corporation, 1943. p 586–622.
9. Kirkwood JG. Theory of solutions of molecules containing widely separated charges with special application to zwitterions. *J Chem Phys* 1934;2:351–361.
  10. Tanford C, Kirkwood JG. Theory of protein titration curves. I. General equations for impenetrable spheres. *J Am Chem Soc* 1957;79:5333–5339.
  11. Zhou H-X. Brownian dynamics study of the influences of electrostatic interaction and diffusion on protein-protein association kinetics. *Biophys J* 1993;64:1711–1726.
  12. Collins KD, Washabaugh MW. The Hofmeister effect and the behavior of water at interfaces. *Q. Rev. Biophys.* 1985;18:323–422.
  13. Onsager L, Samaris NNT. The surface tension of Debye-Hückel electrolytes. *J Chem Phys* 1934;2:528–536.
  14. Wagner C. The surface tension of dilute solutions of electrolytes. *Phys Z* 1924;25:474–477.
  15. Washabaugh MW, Collins KD. The systematic characterization by aqueous chromatography of solutes which affect protein stability. *J Biol Chem* 1986;261:12477–12485.
  16. von Hippel PH, Wong K-Y. On the conformational stability of globular proteins. The effects of various electrolytes and nonelectrolytes on the thermal ribonuclease transition. *J Biol Chem* 1965;240:3909–3923.
  17. Perl D, Schmid FX. Electrostatic stabilization of a thermophilic cold shock protein. *J Mol Biol* 2001;313:343–357.
  18. Ramos CH, Baldwin RL. Sulfate anion stabilization of native ribonuclease A both by anion binding and by the Hofmeister effect. *Protein Sci* 2002;11:1771–1778.
  19. Perez-Jimenez R, Godoy-Ruiz R, Ibarra-Molero B, Sanchez-Ruiz JM. The efficiency of different salts to screen charge interactions in proteins: A Hofmeister effect? *Biophys J* 2004;86:2414–2429.
  20. Zhou H-X, Dong F. Electrostatic contributions to the stability of a thermophilic cold shock protein. *Biophys J* 2003;84:2216–2222.
  21. Zhou H-X. Macromolecular electrostatic energy within the nonlinear Poisson-Boltzmann equation. *J Chem Phys* 1994;100:3152–3162.
  22. Sharp KA, Honig B. Calculating total electrostatic energies with the nonlinear Poisson-Boltzmann equation. *J Phys Chem* 1990;94:7684–7692.
  23. Chen T, Hefter G, Buchner R. Dielectric spectroscopy of aqueous solutions of KCl and CsCl. *J Phys Chem A* 2003;107:4025–4031.
  24. Madura JD, Briggs JM, Wade RC, Davis ME, Luty BA, Ilin A, Antosiewicz J, Gilson MK, Bagheri B, Scott LR, et al. Electrostatics and diffusion of molecules in solution: simulations with the University of Houston Brownian Dynamics program. *Comput Phys Commun* 1995;91:57–95.
  25. Mueser TC, Rogers PH, Arnone A. Interface sliding as illustrated by the multiple quaternary structures of liganded hemoglobin. *Biochemistry* 2000;39:15353–15364.
  26. Brooks BR, Brucoleri RE, Olafson BD, States DJ, Swaminathan S, Karplus M. CHARMM: a program for macromolecular energy, minimization, and dynamics calculations. *J Comput Chem* 1983;4:187–217.
  27. Tanford C. *Physical chemistry of macromolecules*. New York: John Wiley & Sons, Inc.; 1961.
  28. Gibbs JW. On the equilibrium of heterogeneous substances. In: Longley WR, Van Name RG, editors. *The collected works of J. Willard Gibbs*, 1st ed. pp. 434. New York: Longmans, Green and Co.; 1928.
  29. Johansson K, Eriksson JC.  $\gamma$  and  $d\gamma/d\tau$  measurements on aqueous solutions of 1,1-electrolytes. *J Colloid Interface Sci* 1974;49:469–480.
  30. Bhuiyan LB, Bratko D, Outhwaite CW. Electrolyte surface tension in the modified Poisson-Boltzmann approximation. *J Phys Chem* 1991;95:336–340.
  31. Levin Y, Flores-Mena JE. Surface tension of strong electrolytes. *Europhys Lett* 2001;56:187–192.
  32. Ohshima H, Matsubara H. Surface tension of electrolyte solutions. *Colloid Polym Sci* 2004;282:1044–1048.
  33. Jarvis NL, Scheiman MA. Surface potentials of aqueous electrolyte solutions. *J Phys Chem* 1968;72:74–78.
  34. Weissenborn PK, Pugh RJ. Surface tension of aqueous solutions of electrolytes: relationship with ion hydration, oxygen solubility, and bubble coalescence. *J Colloid Interface Sci* 1996;184:550–563.
  35. Bostrom M, Williams DRM, Ninham BW. Surface tension of electrolytes: specific ion effects explained by dispersion forces. *Langmuir* 2001;17:4475–4478.
  36. Zhou H-X. A Gaussian-chain model for treating residual charge-charge interactions in the unfolded state of proteins. *Proc Natl Acad Sci USA* 2002;99:3569–3574.
  37. Dominy BN, Perl D, Schmid FX, Brooks CLr. The effects of ionic strength on protein stability: the cold shock protein family. *J Mol Biol* 2002;319:541–554.
  38. Spencer DS, Xu K, Logan TM, Zhou H-X. Effects of pH, salt, and macromolecular crowding on the stability of FK506-binding protein: an integrated experimental and theoretical study. *J Mol Biol* 2005;351:219–232.
  39. Chitra R, Smith PE. Molecular dynamics simulations of the properties of cosolvent solutions. *J Phys Chem B* 2000;104:5854–5864.
  40. Kalra A, Tugcu N, Cramer SM, Garde S. 2001. Salting-in and salting-out of hydrophobic solutes in aqueous salt solutions. *J Phys Chem B* 105:6380–6386.
  41. Hribar B, Southall NT, Vlachy V, Dill KA. How ions affect the structure of water. *J Am Chem Soc* 2002;124:12302–12311.
  42. Jungwirth P, Tobias DJ. Ions at air/water interface. *J Phys Chem B* 2002;106:6361–6373.
  43. Bhatt D, Newman J, Radke CJ. Molecular dynamics simulations of surface tensions of aqueous electrolytic solutions. *J Phys Chem B* 2004;108:9077–9084.
  44. Mason PE, Neilson GW, Ednderby JE, Saboungi M-L, Dempsey CE, MacKerell ADJ, Brady JW. The structure of aqueous guanidinium chloride solution. *J Am Chem Soc* 2004;126:11462–11470.